


## ORIGINAL RESEARCH ARTICLE

## Eco-Friendly Fabrication and Characterization of ZnO Nanoparticles, PANI, and ZnO-PANI Nanocomposites

Sulaiman Babayo Ali<sup>1,2</sup> , Auwal Adamu Mahmoud<sup>1</sup>, Dahiru Adamu Ajiya<sup>1</sup>, Istifanus Yarkasuwa Chindo<sup>1</sup>, and Bashir Musa<sup>3</sup>

<sup>1</sup>Department of Chemistry, Abubakar Tafawa Balewa University, Bauchi, Nigeria

<sup>2</sup>Department of Chemistry, Nigerian Army University, Biu, Borno State, Nigeria

<sup>3</sup>Department of Chemical Science, Federal University of Kashere, Gombe, State, Nigeria

### ABSTRACT

The increasing presence of organic pollutants, such as dyes and pharmaceutical residues, in water systems poses significant environmental and health risks, requiring the development of effective, sustainable cleanup technologies. In this study, we report the synthesis and detailed characterization of polyaniline (PANI), Zinc oxide (ZnO) nanoparticles, and ZnO/PANI nanocomposites as promising materials for environmental cleanup. The nanocomposites were produced via chemical oxidative polymerization, embedding ZnO nanoparticles within a PANI matrix to enhance their photocatalytic activity. Advanced techniques such as Scanning Electron Microscopy (SEM), Transmission Electron Microscopy (TEM), X-ray Diffraction (XRD), Energy Dispersive X-ray Spectroscopy (EDX), and Brunauer–Emmett–Teller (BET) for surface area analysis were used to explore the structural, morphological, elemental, and surface properties of the individual components and the composite. TEM images showed uniform dispersion of ZnO nanoparticles within the PANI matrix and strong interfacial contact, aiding efficient charge separation. XRD confirmed the formation of a new crystalline phase in the composite and a significant decrease in crystallite size, indicating successful nanocomposite creation. EDX verified the elemental composition and even distribution of Zn, O, C, and N, while BET measurements indicated a notable increase in surface area (235.5 m<sup>2</sup>/g) and optimal pore size (~2.2-2.1 nm) in the nanocomposite compared to the individual components. This research introduces ZnO/PANI nanocomposites as a powerful, scalable material for advanced water treatment, providing a cost-effective and eco-friendly solution for degrading stubborn organic contaminants.

### ARTICLE HISTORY

Received June 13, 2025

Accepted September 04, 2025

Published September 30, 2025

### KEYWORDS

PANI/ZnO Nanocomposites, Nanoparticles, Photocatalyst, Organic contaminants, Wastewater treatment, Characterization.



© The Author(s). This is an Open Access article distributed under the terms of the Creative Commons Attribution 4.0 License [creativecommons.org](https://creativecommons.org/licenses/by-nc/4.0/)

### INTRODUCTION

Nanotechnology is the engineering and manipulation of materials and devices on the nanometer scale (1 to 100 nm). It has radically changed biomedicine, environment, cosmetics, catalysis, etc. (Salata, 2004). One of the main advantages of nanoparticles (NPs) is that their high surface-area-to-volume ratio significantly improves their physical, chemical, and optical properties compared to their bulk counterparts (Belay *et al.*, 2023). Recent studies have demonstrated the effectiveness of nanoparticle incorporation in enhancing the functional properties of original materials enabling enhanced interactions with other molecules (Aliyu *et al.*, 2024; Mahmoud *et al.*, 2025).

Nanoparticles (NPs) may be broadly classified as organic (fullerenes, carbon nanotubes) and inorganic. Research on metal NPs, such as Au, Ag, Pt, and Cu, and metal oxide NPs, such as ZnO and TiO<sub>2</sub>, as well as magnetic NPs, is

gaining increasing interest due to their stability, tunability, and multilayer applications (Eker *et al.*, 2024; Yahaya *et al.*, 2022). Metallic nanoparticles are crucial in several industrial applications due to their unique catalytic, optical, and magnetic properties. Gold nanoparticles appear wine-red due to localized surface plasmon resonance, a feature known for a long time and still used today in diagnostics and material design. (Pluchery *et al.*, 2023).

The synthesis of nanoparticles has evolved through various techniques including solvothermal, sol-gel, hydrothermal, microwave, and ultrasonic methods, each offering control over particle morphology and crystallinity (Mourdikoudis *et al.*, 2018). For instance, solvothermal synthesis is particularly effective for producing uniform and highly crystalline TiO<sub>2</sub> nanoparticles, known for their

**Correspondence:** Sulaiman Babayo Ali. Department of Chemistry, Abubakar Tafawa Balewa University, Bauchi, Nigeria. ✉ [sbali.pg@atbu.edu.ng](mailto:sbali.pg@atbu.edu.ng).

**How to cite:** Ali, S. B., Mahmoud, A. A., Ajiya, D. A., Chindo, I. Y., & Musa, B. (2025). Eco-Friendly Fabrication and Characterization of ZnO Nanoparticles, PANI, and ZnO-PANI Nanocomposites. *UMYU Scientifica*, 4(3), 448 – 457. <https://doi.org/10.56919/usci.2543.044>

photocatalytic activity, chemical inertness, and environmental safety (Nam *et al.*, 2013).

Among metal oxides, ZnO is a multifunctional oxide. It has three crystal forms: wurtzite, zinc blende, and rock salt. The wurtzite structure is the most stable and is invariably used (Kumar *et al.*, 2021). ZnO is an n-type semiconductor with a direct band gap of 3.37 eV. Thus, it is suitable for applications such as UV shielding, solar energy, photocatalysis, and drug delivery systems (Zhu & Wang, 2025). The photocatalytic effectiveness proceeds through four steps: photon absorption and the generation of an electron-hole pair, followed by recombination, reactive species formation, and pollutant degradation. (Paul & Ahmaruzzaman, 2025).

ZnO NRs are being used in various applications due to their exciting morphological, optoelectronic, and catalytic attributes. Several recent investigations highlight successful green synthesis approaches that produce high-purity ZnO nanostructures with desirable physicochemical properties. In accordance with Channa *et al.* (2025), ZnO NRs produced via eco-friendly processes exhibit a crystalline hexagonal wurtzite structure. Additionally, its particle size ranges between 30 nm to more than 100 nm depending on the biomaterials and precursors employed.

The photocatalytic efficiency under UV and visible light irradiation has been validated, with degradation rates for organic dyes such as methylene blue exceeding 90% (Abdullah *et al.*, 2020). Moreover, Metal oxide nanostructures such as ZnO, Fe<sub>3</sub>O<sub>4</sub> etc. modified with polymers like polyaniline show enhanced surface areas and improved photocatalytic activity, attributed to synergistic interactions (Jadoun *et al.*, 2022; Mahmoud *et al.*, 2022).

In addition, the synthesis processes can include plant extracts from *Anacardium occidentale*, *Cocos nucifera*, banana peel, and others. These are effective for nanoparticle synthesis and act as stabilizers and reducing agents (Ajayan & Hebsur, 2020; Rahman *et al.*, 2022). XRD, SEM, TEM, and EDX tests confirmed the structural integrity and elemental purity of these nanostructures. In solar applications, ZnO-coated silver solar cells showed improved fill factor and conversion efficiency. This finding suggests sensitivity to renewables (Danladi *et al.*, 2022). Collectively, these results show that green-synthesized ZnO nanoparticles can be useful for environmental, bio, and energy applications.

## MATERIALS AND METHODS

### Experimental

A Range of analytical grade reagents and solvents from Sigma Aldrich and BDH were used, without further purification. Aniline, HCl, (NH<sub>4</sub>)<sub>2</sub>S<sub>2</sub>O<sub>8</sub>, K<sub>2</sub>S<sub>2</sub>O<sub>8</sub>, NaOH, Zn(CH<sub>3</sub>COO)<sub>2</sub>·2H<sub>2</sub>O, ethanol and deionized water. Banana peels were used as a natural precursor. An

ultrasonic bath and magnetic stirrer were employed for solution preparation and polymerization.

The material characterization was done by the analysis of BET for surface area, XRD (Bruker D8 Advance, Cu-K $\alpha$ , 2 $\theta$  = 30–80°), FESEM (FEI Quanta FEG 650), EDX (JEOL JSM-7600F), and FTIR spectroscopy (PerkinElmer System 2000, KBr pellet, 400–4000 cm<sup>-1</sup>).

### Synthesis of Polyaniline (PAni)

The synthesis of polyaniline (PAni), with slight modifications to the method of (Nabi *et al.*, 2011). A solution of aniline (10% w/v) in water was made and cooled to 10° C. The dropwise addition of potassium persulfate (K<sub>2</sub>S<sub>2</sub>O<sub>8</sub>) in a 1:1 molar ratio (oxidant: aniline) was performed under concurrent Magnetic stirring. After 1 hour of reaction, a dark green gel formed, indicating successful polymerization of PAni.

### Preparation of Banana Peel (BP) Extract

The *Musa spp.* peel (BP) extract was prepared using a modified protocol as described by Abdullah *et al.* (2020). The ripe bananas were bought at Gombe State in Nigeria. The fruit peels were separated and washed by hand with tap water, then with deionized water, and air-dried overnight at room temperature. A total of 100 g of chopped banana peel was added to 300 mL of deionized water and heated to 80 °C for 25 minutes. When the mixture was cooled to room temperature, it was filtered twice using Whatman No. 1 filter paper to give the aqueous extract.

### Green Synthesis of Zinc Oxide (ZnO) Nanoparticles

ZnO nanoparticles were synthesized using a green route adapted from Abdullah *et al.* (2021). A 2 mL aliquot of BP extract was added dropwise to 100 mL of 0.02 M zinc acetate dihydrate solution under magnetic stirring for 20 minutes. The pH was adjusted to 12 by the gradual addition of 2 M NaOH solution. The reaction was allowed to proceed at room temperature with continuous stirring for 3 hours. The resulting white suspension was centrifuged at 3500 rpm for 15 minutes (Kubota Centrifuge, Model 4000, Japan). The precipitate was washed repeatedly with deionized water and absolute ethanol, then dried in a hot air oven at 60 °C overnight to yield ZnO nanoparticles.

### Synthesis of PAni/ZnO Nanocomposite

PAni/ZnO nanocomposite was made using a modified method of (Mostafaei & Zolriasatein, 2012). A stock solution of PAni at 10% was prepared, and 4.5 g of PAni gel was added to a dispersion of 0.9 g ZnO nanoparticles (20 wt.% ZnO) in 200 mL of distilled water. To allow for good mixing and interaction, the mixture was magnetically stirred in an ice-water bath for 4 hours. The greenish gel was left at room temperature (27 °C) for a duration of 24

hours. The liquid on top was discarded; the sample was restored by filtration.

**RESULTS AND DISCUSSION**

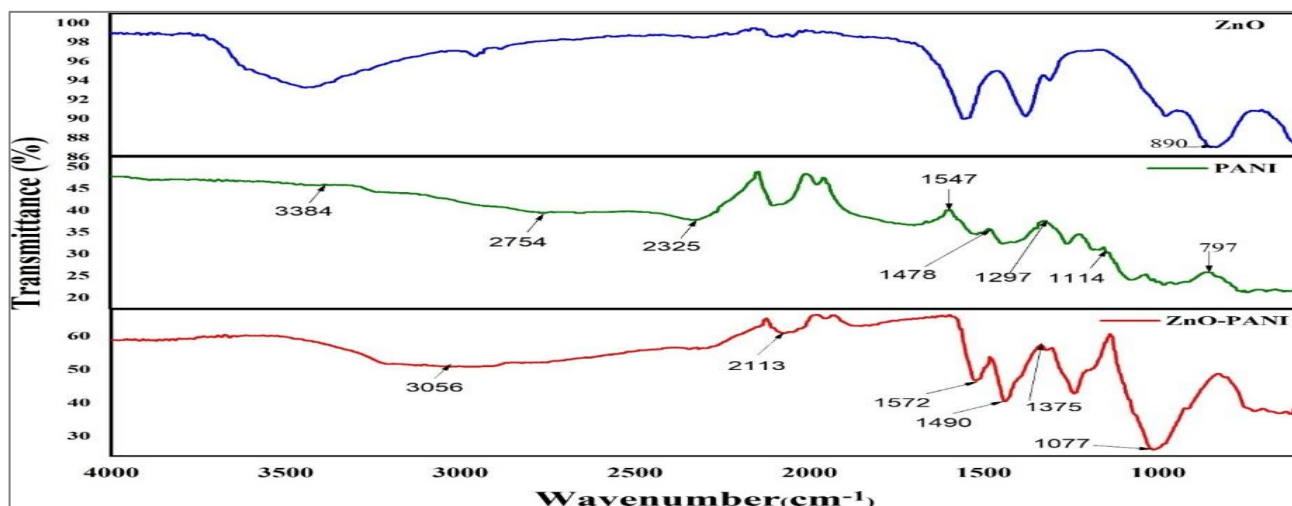


Figure 1: FTIR spectra of Polyaniiline (PANI), ZnO Nanoparticles and ZnO/PANI Nanocomposite

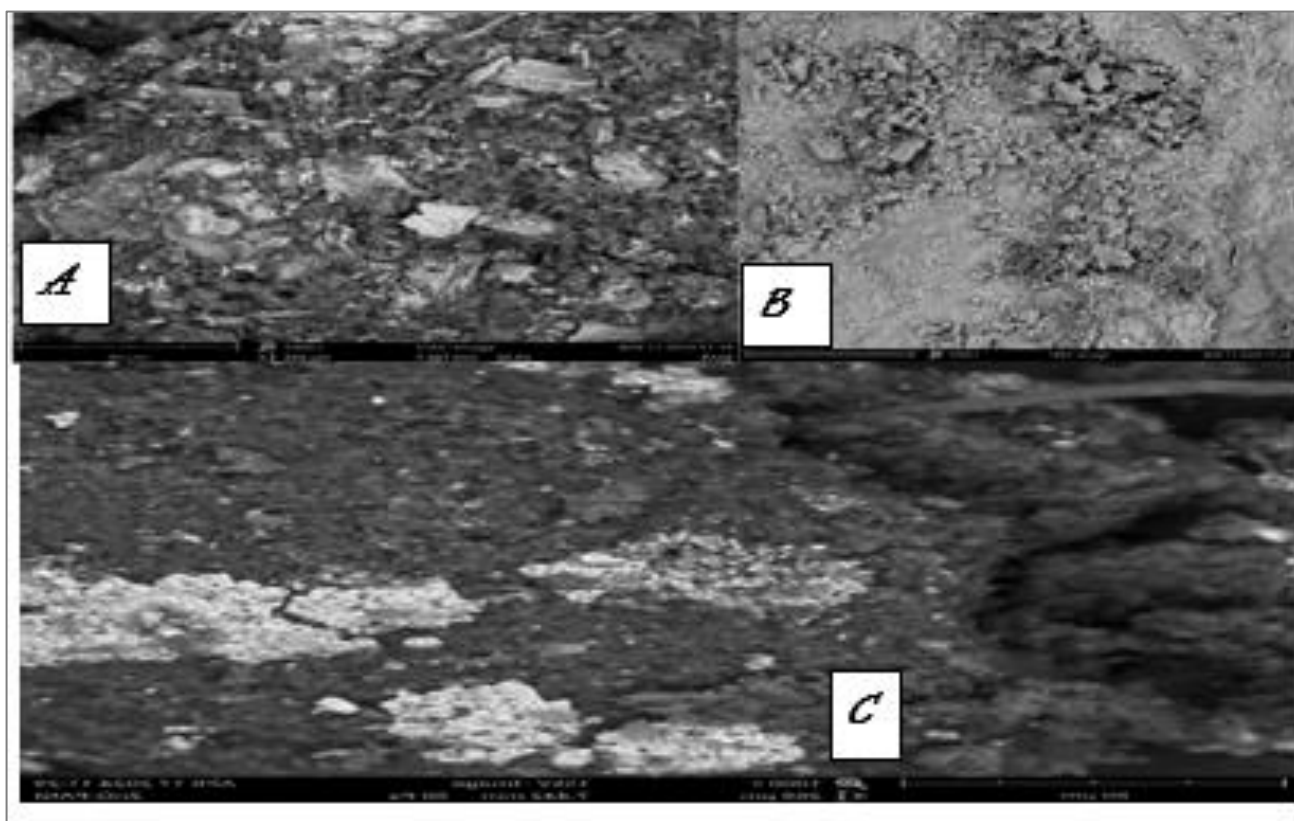


Figure 2: SEM Micrographs of (A) Polyaniiline (PANI), (B) ZnO Nanoparticles and (C) ZnO/PANI Nanocomposite at X1000 magnification.

**FTIR Analysis of ZnO/PANI Nanocomposites**

**FTIR Characterization of ZnO, PANI, and PANI/ZnO Nanocomposite**

The Fourier-transform infrared (FTIR) spectrum of the synthesized ZnO nanoparticles shows an adsorption band near 890  $\text{cm}^{-1}$  (Figure 1), which corresponds to Zn–O stretching, thus confirming the formation of ZnO (Srimeena & Nithya, 2019).

In contrast, the FTIR spectrum of pure polyaniline (PANI) reveals several characteristic absorption bands associated with its molecular structure:

The FTIR spectrum shows a band at 3384  $\text{cm}^{-1}$  corresponding to the N–H stretching vibration of an amine, and a band at 3056  $\text{cm}^{-1}$  assigned to the C–H in-plane bending vibration of an aromatic ring. According to the peaks 1547 and 1478  $\text{cm}^{-1}$  corresponding to C=N and C=C stretching vibrations (Adamu *et al.*, 2015). They are due to the quinoid and benzenoid structures associated

with the conductive emeraldine form of PANI. Moreover, the signals at 1297  $\text{cm}^{-1}$ , 1114  $\text{cm}^{-1}$ , and 797  $\text{cm}^{-1}$  are attributed to C–H stretching and bending vibrations in the polymer backbone (Jarad *et al.*, 2016; Mahmoud *et al.*, 2025).

The spectrum (FTIR) of PANI/ZnO shows bands that ZnO owns and PANI, which were put on the surface.

The presence of Zn evidences the effective incorporation of ZnO nanoparticles–O stretching band at 890  $\text{cm}^{-1}$ . In the meantime, the key PANI bands at 3384  $\text{cm}^{-1}$ , 3056  $\text{cm}^{-1}$ , 1547  $\text{cm}^{-1}$ , and 1478  $\text{cm}^{-1}$  show very little shift, indicating the functional groups of PANI are retained in the composite matrix. It demonstrates that the PANI structure is compatible and that its conductivity is retained after composite formation.

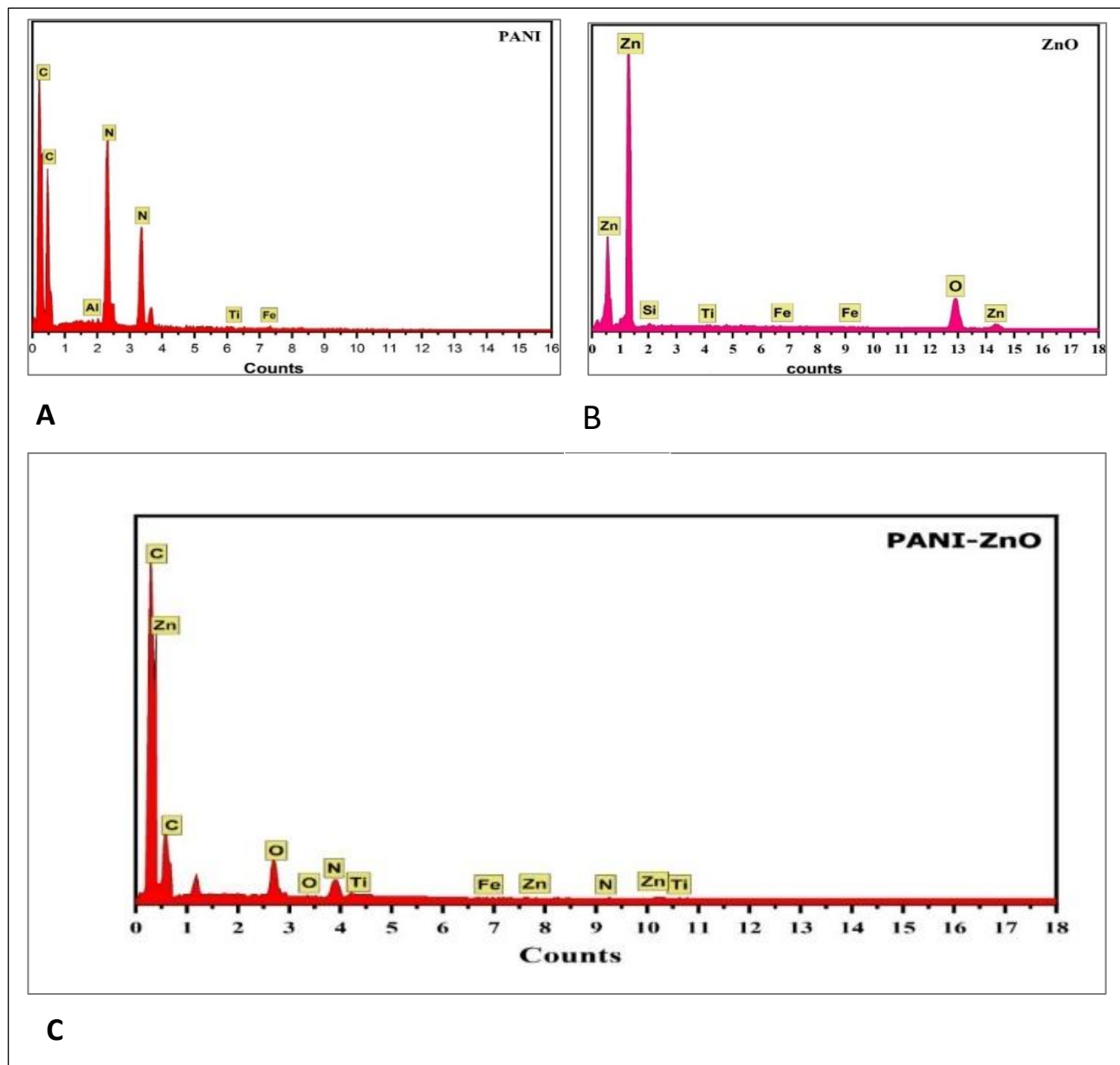


Figure 3: EDX results of (A) Polyaniline (PANI), (B) ZnO Nanoparticles, and (C) ZnO/PANI Nanocomposite

Table 1: XRD Properties of ZnO Nanoparticles, Polyaniline, and ZnO/PANI Nanocomposites

| Nanomaterial | Peak position ( $^{\circ}2\theta$ ) | d-Spacing ( $\text{\AA}$ ) | FWHM   | Crystallite Size | Phase              | Nature               |
|--------------|-------------------------------------|----------------------------|--------|------------------|--------------------|----------------------|
| ZnO          | 36.5574                             | 2.45804                    | 0.3936 | 21.5             | Hexagonal Wurtzite | n-type Semiconductor |
| PANI         | 27.7700                             | 3.21259                    | 0.0984 | 46.04            | Semi Crystallite   | Conducting Polymer   |
| ZnO/PANI     | 21.3389                             | 4.16041                    | 0.2755 | 28.8             | Hybrid Composite   | Hybrid Semiconductor |

Also, slight shifts and new absorption features observed in the ZnO/PANI nanocomposite spectra suggest the presence of intermolecular interactions between ZnO and PANI. Moreover, this may be due to hydrogen bonding or coordination interactions. When these molecules interact with the photocatalyst, then electron transport is enhanced. There is also a reduction in charge-carrier recombination.

These results align with previous studies (Sharma *et al.*, 2016), which reported comparable spectral features and noted the retention and shifting of FTIR bands upon composite formation. Similarly, Mehto *et al.* (2016) observed interaction-induced modifications in PANI/ZnO composites, supporting the findings of this study.

The functional groups identified by FTIR analysis are critical to the composite's photocatalytic activity. They not only contribute active sites for pollutant adsorption and degradation but also enhance interfacial charge transfer between ZnO and PANI. Liu *et al.* (2014) emphasized the role of such interactions in improving the photocatalytic degradation of organic dyes, reinforcing the relevance of the observed FTIR features in the current study.

FTIR spectroscopy confirms the successful synthesis of the PANI/ZnO nanocomposite and reveals significant molecular interactions between the components. These interactions, along with the preserved functional groups, contribute to the material's overall structural integrity and functional performance.

## SEM Analysis of Polyaniline (PANI), ZnO Nanoparticles, and ZnO/PANI Nanocomposites

### Scanning Electron Microscopy (SEM) Analysis

Scanning Electron Microscopy (SEM) provides detailed visualization of the surface morphology and microstructural characteristics of nanomaterials, which are essential for understanding their functional properties, particularly in photocatalytic applications. Figure 2A–C present SEM micrographs of polyaniline (PANI), ZnO nanoparticles, and the ZnO/PANI nanocomposite, respectively, offering a comparative insight into their individual and composite morphologies.

### Surface Morphology and Texture

At a 1000 magnification, PANI (Plate A) possesses a rough and granular appearance with a morphology that is irregular and agglomerated. These features are intrinsic to the PANI polymeric chain structure and therefore provide many active surface sites that readily interact with ZnO during composite formation. On the other hand, ZnO nanoparticles (Plate B) possess a more uniform quasi-spherical shape with a smooth, well-defined surface, resulting in a greater specific surface area and greater availability of reactive sites. The morphology of

ZnO/PANI nanocomposite (Plate C) is homogeneous and integrated as the ZnO (zinc oxide) nanoparticles are uniformly scattered and embedded in the PANI (Polyaniline) matrix, confirming the successful formation of the composite to establish strong physical interactions with good dispersion. Good dispersion is important for enhancing charge separation and facilitating effective electron transfer.

### Interfacial Interactions and Structural Integrity

The nanostructure of the ZnO/PANI nanocomposite consists of well-distributed ZnO nanocrystals in a PANI matrix, as indicated by SEM images, suggesting a strong interaction between ZnO and PANI. The strong linkage helps separate the electrons and holes more efficiently, reduces recombination (which is good), and enhances the photocatalytic performance of the material. Because the structure is continuous and well-connected, this suggests that the nanoparticles remain uniformly dispersed throughout the structure, without agglomerating, phase separating, or occupying multiple regions.

### Comparative Literature Support

These SEM findings corroborate recent reports in the literature:

Multiple studies show that structural and morphological features can enhance the photocatalytic performance of PANI/ZnO composites. Turkten *et al.* (2021) emphasize that photocatalytic efficiency can be improved by achieving a uniform distribution of nanoparticles. Scholars found that careful control of surface morphology can enhance photocatalytic activity (Chen *et al.*, 2020). Structural integrity is essential for long-term stability and sustained performance (Kasak, 2024). Navidpour *et al.* (2024) showed that well-made composites can exhibit improved degradation of pharmaceutical pollutants due to suitable charge transfer and a uniform structure throughout the nanocomposite.

### EDX Analysis of Polyaniline (PANI), ZnO Nanoparticles, and ZnO/PANI Nanocomposites

The elemental composition and distribution of materials are determined using Energy Dispersive X-ray Spectroscopy (EDX). EDX spectra and elemental mapping were used to characterize pure polyaniline (PANI), ZnO nanoparticles, and ZnO/PANI nanocomposites. Analysis of samples for elemental identity, compositional purity, and material homogeneity is an important parameter for optimizing photocatalytic performance.

The EDX spectrum of ZnO nanoparticles displays sharp peaks for zinc (Zn) and oxygen (O) as shown in Figure 3. This confirms the successful and pure synthesis of ZnO, and their elemental ratios confirm the expected ZnO ratios. The EDX peaks of polyaniline (PANI) reveal carbon (C) and nitrogen (N). This is characteristic of its polymer backbone and indicates its successful synthesis.

The EDX spectrum of the ZnO/PANI nanocomposite shows characteristic peaks for Zn, O, C, and N,

confirming effective anchoring and dispersion of ZnO nanoparticles during PANI polymerization.

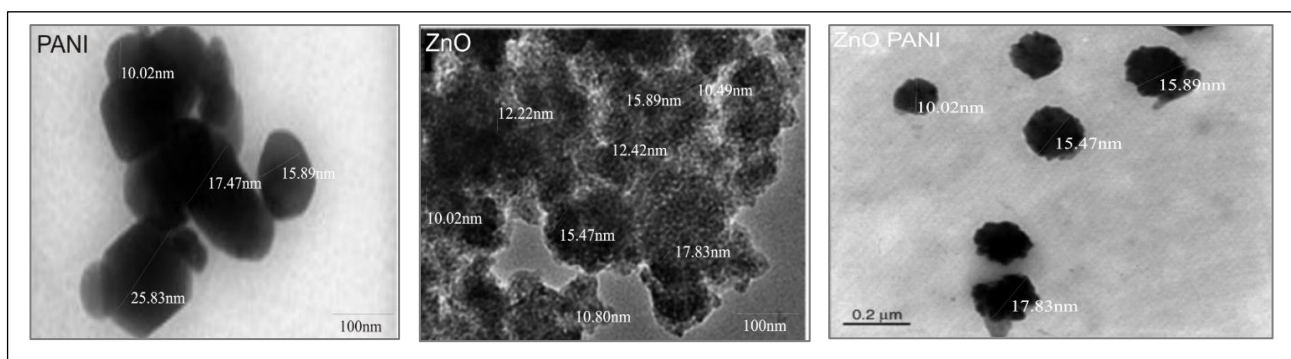


Figure 4: TEM Micrographs of Polyaniline (PANI), ZnO Nanoparticles, and ZnO/PANI Nanocomposite

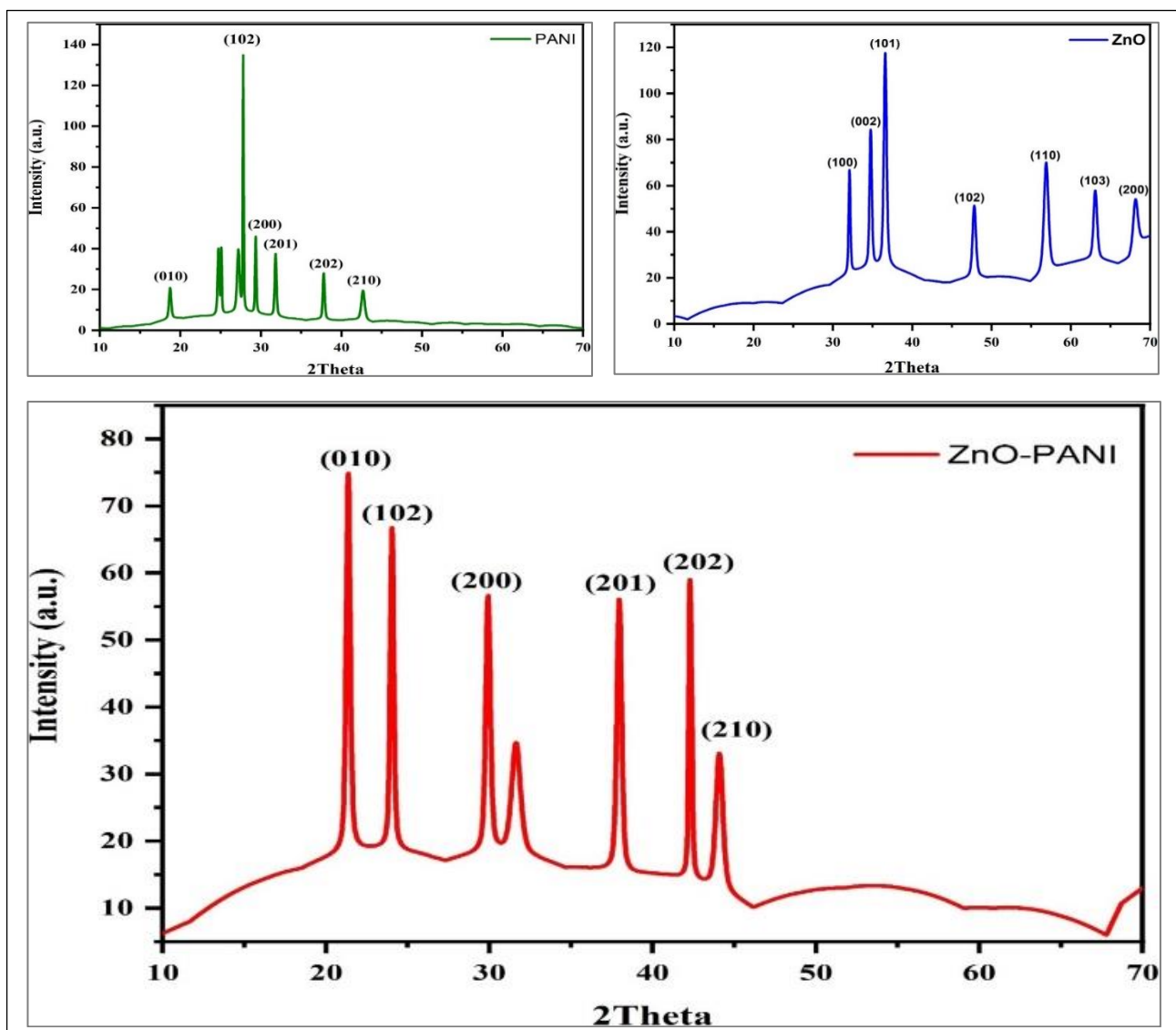


Figure 5: XRD Pattern of (a) Polyaniline (PANI), (b) ZnO Nanoparticles, and (c) ZnO/PANI Nanocomposite

### Quantitative Elemental Analysis

The EDX analysis of the ZnO nanoparticles showed very high Zn and O contents, with other elements negligible. In contrast, the ZnO/PANI nanocomposite has lower weight percentages of Zn and O but higher amounts of C and N, which indicate the presence of PANI in the composite. The reduction of Zn and O content with

respect to pure ZnO is consistent with the expected mixed composition of the nanocomposite.

### Comparison with Literature and Photocatalytic Relevance

Zhanfeng *et al.* (2025) emphasize the critical role of uniform elemental distribution and balanced composite

composition in enhancing photocatalytic performance, which aligns with the current findings. Similarly, [Turkten et al. \(2021\)](#) reported significant improvements in the photocatalytic degradation of organic dyes using PANI/ZnO nanocomposites, attributing this enhancement to optimized elemental dispersion and synergistic interactions between the PANI and ZnO phases.

### TEM Analysis for PANI, ZnO Nanoparticles, and ZnO/PANI Nanocomposites

Transmission Electron Microscopy (TEM) was utilized to investigate the morphology, size distribution, crystallinity, and interfacial structure of polyaniline (PANI), ZnO nanoparticles, and their nanocomposites ([Figure 4](#)). The results reveal critical structural features that underpin the enhanced photocatalytic performance of these materials.

#### ZnO Nanoparticles.

The ZnO nanoparticles uniformly take a quasi-spherical nature throughout the samples. Moreover, uniformity promotes efficient interactions with the pollutant during photocatalysis, owing to its surface area-to-volume ratio. Furthermore, the nanoparticles' crystalline structure is of high quality, with limited defects. Thus, electron transport is easy in the particles. Therefore, efficient photocatalytic performance is due to important factors that enable efficient electron transport within the nanoparticles.

#### ZnO/PANI Nanocomposites.

The TEM analysis suggests that ZnO nanoparticles are embedded within the PANI matrix. The close contact between ZnO and PANI indicates strong interfacial bonding, which facilitates efficient charge separation and transfer, thereby slowing electron-hole recombination and enhancing photocatalytic activity. Moreover, amorphous regions formed by PANI can act as trapping sites for the photogenerated charge carriers, thereby improving their lifetimes and enhancing the degradation efficiency.

#### Correlation with Literature

According to [Wang et al. \(2025\)](#), to improve photocatalytic performance, it is important to achieve morphological uniformity and strong interfacial bonding. Furthermore, [Wang et al. \(2021\)](#) reported that the presence of an amorphous region is useful for trapping charge carriers, thereby further improving photocatalytic performance. [Qu et al. \(2025\)](#) also demonstrated that the activity of smaller, uniformly distributed nanoparticles is higher due to greater surface exposure. Based on these findings, it was observed that the photocatalytic degradation of methylene blue was more pronounced for ZnO/PANI composites than for pure ZnO ([Zhou et al. 2025](#)).

### XRD Analysis Summary for Polyaniline (PANI), ZnO Nanoparticles, and ZnO/PANI Nanocomposites

X-ray Diffraction (XRD) analysis provides vital insights into the crystalline structure, phase composition, and crystallite size of nanomaterials. The diffraction patterns depicted in [Figure 5](#) and [Table 1](#) reveal significant structural features of pure polyaniline (PANI), ZnO nanoparticles, and ZnO/PANI nanocomposites, which are critical for optimizing their photocatalytic performance.

#### Observations:

The composite shows a marked shift in the peak position compared to both pure ZnO and PANI. Also, the peak widening points towards a new phase of interaction between the two components. The observations confirm the successful formation of ZnO-PANI composite with strong interfacial interactions.

#### Structural Implications

The photocatalytic activity increases as the surface area increases when the crystallite size of ZnO is reduced below its bulk size. The ZnO/PANI nanocomposite exhibits a slightly larger crystallite size compared to pure ZnO, which can be attributed to the slight reordering that happens during composite preparation. Thus, the two materials undergo structural changes. Moreover, the increase in the composite's d-spacing indicates lattice expansion, which may be due to strong interface contact between ZnO and PANI, leading to efficient charge separation and transfer. In addition, a new diffraction peak in the XRD pattern was observed, indicating that there is no physical mixture and that an interaction-driven phase is generated. Consequently, the material exhibits synergy, transforming its structural and functional properties.

#### Correlation with Literature

Literature studies support structural observations. [Eskizeybek et al. \(2012\)](#) indicate that the peak shift and crystallite size reduction for PANI/ZnO nanocomposite were similar and corresponded with what was observed here. Moreover, [Tababouchet et al. \(2023\)](#) stated that these peak shifts and d-spacing increment were due to the strong integrity of the composite and structural compatibility of the constituent phases. Thus, the introduction of composites leads to lattice expansion. [Kumar et al. \(2023\)](#) reported that enhanced photocatalytic degradation performance is due to well-controlled crystallite size and improved ordering associated with the optimized crystallographic features of the ZnO/PANI composite. As such, structural modifications are believed to be highly functional.

## BET Analysis for Polyaniline (PANI), ZnO Nanoparticles, and ZnO/PANI Nanocomposites

The Brunauer–Emmett–Teller (BET) analysis offers crucial insights into the specific surface area, pore size, and porosity of nanomaterials, key parameters that influence photocatalytic and adsorption performance. Table 2 summarizes the BET results for ZnO nanoparticles, PANI, and their ZnO/PANI nanocomposite, demonstrating how composite formation enhances surface characteristics.

**Table 2: BET results of ZnO/PANI**

| Sample.  | SA (m <sup>2</sup> /g) | Pore size (nm) |
|----------|------------------------|----------------|
| ZnO      | 142.510                | 2.136          |
| PANI     | 211.494                | 2.132          |
| ZnO/PANI | 235.505                | 2.128          |

**Key: SA = Surface area**

### ZnO Nanoparticles

The material exhibits a high surface area of 142.510 m<sup>2</sup>/g, which is attributed to its nanoscale particle size and is highly advantageous for both photocatalytic and adsorption-based applications. The measured pore diameter of approximately 2.136 nm places the material within the mesoporous range, further supporting efficient diffusion and interaction of reactant molecules within the structure. These textural features collectively enhance the composite's functional performance; however, partial nanoparticle agglomeration cannot be ruled out and may reduce the effective surface area available for catalytic activity.

### Polyaniline (PANI)

Pollutants can easily get into makeup, and ions can travel quickly. The composite has a significantly greater surface area of 211.494 m<sup>2</sup>/g compared to pure ZnO. This is due to the fibrous, porous nature of the polymeric PANI network. The 2.132 nm pore size is just sufficient for many polymers to enter the pore. By incorporating a structurally porous framework into the composite, it has greater adsorption capacity to capture pollutants and better charge-transport functionality, which helps improve the composite's performance.

### ZnO/PANI Nanocomposite

The ZnO/PANI nanocomposite has the highest surface area of the samples at 235.505 m<sup>2</sup>/g, indicating the synergistic effect of ZnO incorporation in the polymer matrix. The pore size of 2.128 nm indicates uniform mesoporosity, which is appropriate for adsorption and molecular diffusion. Embedding ZnO nanoparticles in the PANI network will control their agglomeration, promote better dispersion throughout the matrix, improve porosity and surface area, and enhance adsorption and photocatalytic performance.

## Correlation with Literature

According to literature reports, the ZnO/PANI nanocomposite showed structural and functional benefits. Gilja *et al.* (2018) observed the same increase in BET surface area due to strong interactions between PANI and ZnO, which improved their photocatalytic performance. According to He *et al.* (2022), for efficient pollutant degradation, high surface area and pore volume are necessary in ZnO-based composites. Moreover, the analysis using the Barrett–Joyner–Halenda (BJH) method confirms the mesoporous nature of all samples, with the ZnO/PANI composite demonstrating an even pore-size distribution, which allows rapid adsorption and molecular diffusion, highlighting its great functional properties.

## CONCLUSION

These results highlight the potential of ZnO/PANI nanocomposites as efficient, sustainable nanomaterials with superior structural and functional properties. This research focuses on PANI/ZnO nanocomposites and their characterization. By finding a PANI matrix that improves the structural, morphological, and surface properties of the ZnO nanoparticles added to it. According to TEM analyses, the structure of the studied materials appears well-dispersed, exhibiting a network-like formation; this implies strong interfacial interactions between ZnO and PANI. Hence, high interaction leads to improved stability and performance of the materials. According to the XRD results, a new crystalline phase formed, accompanied by a decrease in crystallite size due to the synergistic interaction of the constituents. The BET analysis showed that there is more surface area and pores of optimal size, which provide many active sites. Due to these improved characteristics, the nanocomposite may be suitable for future applications, such as photocatalytic degradation, thanks to its increased surface area and enhanced properties.

## REFERENCE

- Abdullah, F. H., Abu Bakar, N. H. H., & Abu Bakar, M. (2020). Low temperature biosynthesis of crystalline zinc oxide nanoparticles from *Musa acuminata* peel extract for visible-light degradation of methylene blue. *Optik*, 206, 164279. [Crossref]
- Abdullah, F. H., Abu Bakar, N. H. H., & Abu Bakar, M. (2021). Comparative study of chemically synthesized and low temperature bio-inspired *Musa acuminata* peel extract mediated zinc oxide nanoparticles for enhanced visible-photocatalytic degradation of organic contaminants in wastewater treatment. *Journal of Hazardous Materials*, 406, 124779. [Crossref]
- Adamu, M. A., Mustafa, M. K., & Ruslan, N. N. (2015). Morphology of Polyaniline nanotube with various level of Fe<sub>3</sub>O<sub>4</sub> nanoparticles and their electrical conductivities by Ultrasonic dispersion method. *Journal of Engineering and Applied Sciences*, 11(16), 9725-9729.

- Ajayan, A. S., & Hebsur, N. S. (2020). Green synthesis of zinc oxide nanoparticles using neem (*Azadirachta indica*) and tulasi (*Ocimum tenuiflorum*) leaf extract and their characterization. *International Journal of Current Microbiology and Applied Sciences*, 9(2), 277–285. [Crossref]
- Aliyu, A., Umar, S., Abdelmalik, A. A., Abdulsalam, H., Maidawa, S. S., & Suleiman, S. A. (2024). Effect of silica and alumina nanoparticles addition on the dielectric and rheological properties of shea oil methyl ester. *UMYU Scientifica*, 3(2), 70–75. [Crossref]
- Belay, T., Worku, L. A., Bachheti, R. K., Bachheti, A., & Husen, A. (2023). Nanomaterials: Introduction, synthesis, characterization, and applications. In A. Husen (Ed.), *Advances in Smart Nanomaterials and Their Applications* (pp. 1–21). Academic Press. [Crossref]
- Channa, G. M., Iturbe-Ek, J., Sustaita, A. O., Melo-Maximo, D. V., Bhatti, A., Esparza-Sanchez, J., Navarro-Lopez, D. E., Lopez-Mena, E. R., Sanchez-Lopez, A. L., & Lozano, L. M. (2025). Eco-friendly synthesis of ZnO nanoparticles from natural agave, chiku, and soursop extracts: A sustainable approach to antibacterial applications. *Crystals*, 15(5), 470. [Crossref]
- Chen, D., Cheng, Y., Zhou, N., Chen, P., Wang, Y., Li, K., Huo, S., Cheng, P., Peng, P., Zhang, R., Wang, L., Liu, H., Liu, Y., & Ruan, R. (2020). Photocatalytic degradation of organic pollutants using TiO<sub>2</sub>-based photocatalysts: A review. *Journal of Cleaner Production*, 268, 121725. [Crossref]
- Danladi, E., Onimisi, M. Y., Laah, R. M., & Ikhioya, I. L. (2022). High performance dye sensitized solar cells by plasmonic enhancement of silver nanoparticles in ZnO photoelectrode with betanin pigment. *African Scientific Reports*, 1(1), 1–15. [Crossref]
- Eker, F., Duman, H., Akdaşçı, E., Bolat, E., Sarıtaş, S., Karav, S., & Witkowska, A. M. (2024). A comprehensive review of nanoparticles: From classification to application and toxicity. *Molecules*, 29(15), 3482. [Crossref]
- Eskizybek, V., Sari, F., Gülce, H., Gülce, A., & Avcı, A. (2012). Preparation of the new polyaniline/ZnO nanocomposite and its photocatalytic activity for degradation of methylene blue and malachite green dyes under UV and natural sun lights irradiations. *Applied Catalysis B: Environmental*, 119–120, 197–206. [Crossref]
- Gilja, V., Vrban, I., Mandić, V., Žic, M., & Hrnjak-Murgić, Z. (2018). Preparation of a PANI/ZnO composite for efficient photocatalytic degradation of acid blue. *Polymers*, 10(9), 940. [Crossref]
- He, X., Yang, Y., Li, Y., Chen, J., Yang, S., Liu, R., & Xu, Z. (2022). Effects of structure and surface properties on the performance of ZnO towards photocatalytic degradation of methylene blue. *Applied Surface Science*, 599, 153898. [Crossref]
- Jadoun, S., Yáñez, J., Mansilla, H. D., Riaz, U., & Chauhan, N. P. S. (2022). Conducting polymers/zinc oxide-based photocatalysts for environmental remediation: A review. *Environmental Chemistry Letters*, 20(3), 2063–2083. [Crossref]
- Jarad, A. N., Ibrahim, K., & Ahmed, N. M. (2016). Synthesis and characterization thin films of conductive polymer (PANI) for optoelectronic device application. *AIP Conference Proceedings*, 1733(1), 020010. [Crossref]
- Kasak, P. (2024). Degradation and photocatalytic properties of nanocomposites. *Nanomaterials*, 14(13), 1065. [Crossref]
- Kumar, H., Luthra, M., Punia, M., Yadav, A., Kumari, R., Sharma, R., Tundwal, A., Kumar, G., & Kaur, P. (2023). PANI encapsulated  $\alpha$ -MnO<sub>2</sub> nanocomposites as photocatalytic, antibacterial and anticorrosive agents: Sustainable experimental and theoretical studies. *Results in Engineering*, 19, 101250. [Crossref]
- Kumar, S., Awasthi, K., & Mishra, Y. K. (2021). Synthesis of ZnO nanostructures. In K. Awasthi (Ed.), *Nanostructured Zinc Oxide: Synthesis, Properties and Applications* (pp. 93–116). Elsevier. [Crossref]
- Liu, B., Zhao, X., Terashima, C., Fujishima, A., & Nakata, K. (2014). Thermodynamic and kinetic analysis of heterogeneous photocatalysis for semiconductor systems. *Physical Chemistry Chemical Physics*, 16(19), 8751–8760. [Crossref]
- Mahmoud, A. A., Ali, S. B., Ajiya, D. A. & Muhammad, M. (2025). Photodegradation of some Antibiotics and Industrial Dye by Visible Light of Highly Active Synthesized PAni/TiO<sub>2</sub> Nanocomposite Photocatalyst. *Journal of Bio & Geo Material and Energy*, 5 (1), 28-38. [Crossref]
- Mahmoud, A. A., Mustafa, M. K., Ruslan, N. N., Aliyu, J., Garba, I. H. & Hassan, U. F. (2022). Amperometric immunosensor based on the conducting layer of PANi/Fe<sub>3</sub>O<sub>4</sub> nanocomposites for the detection of A $\beta$ 42. *Science Forum Journal of Pure and Applied Sciences*. 22 326 - 335. [Crossref]
- Mehto, V. R., Mehto, A., Gupta, D. K., & Pandey, R. K. (2016). Synthesis and characterization of PANI/ZnO nanocomposites. *Journal of the Chinese Chemical Society*, 63(11), 935–946. [Crossref]
- Mostafaei, A., & Zolriasatein, A. (2012). Synthesis and characterization of conducting polyaniline nanocomposites containing ZnO nanorods. *Progress in Natural Science: Materials International*, 22(4), 273–280. [Crossref]
- Mourdikoudis, S., Pallares, R. M., & Thanh, N. T. K. (2018). Characterization techniques for nanoparticles: Comparison and complementarity upon studying nanoparticle properties. *Nanoscale*, 10(27), 12871–12934. [Crossref]
- Nabi, S. A., Shahadat, M., Bushra, R., Oves, M., & Ahmed, F. (2011). Synthesis and characterization of polyanilineZr(IV)sulphosalicylate composite and its applications (1) electrical conductivity, and (2)

- antimicrobial activity studies. *Chemical Engineering Journal*, 173(3), 706–714. [\[Crossref\]](#)
- Nam, C. T., Yang, W. D., & Duc, L. M. (2013). Solvothermal synthesis of TiO<sub>2</sub> photocatalysts in ketone solvents with low boiling points. *Journal of Nanomaterials*, 2013(1), 627385. [\[Crossref\]](#)
- Navidpour, A. H., Ahmed, M. B., & Zhou, J. L. (2024). Photocatalytic degradation of pharmaceutical residues from water and sewage effluent using different TiO<sub>2</sub> nanomaterials. *Nanomaterials*, 14(2), 135. [\[Crossref\]](#)
- Paul, R. K., & Ahmaruzzaman, M. (2025). Advanced photocatalytic degradation of POPs and other contaminants: A comprehensive review on nanocomposites and heterojunctions. *RSC Advances*, 15(38), 31313–31359. [\[Crossref\]](#)
- Pluchery, O., Prado, Y., & Watkins, W. (2023). A complete explanation of the plasmonic colours of gold nanoparticles and of the bichromatic effect. *Journal of Materials Chemistry C*, 11(45), 15824–15832. [\[Crossref\]](#)
- Qu, B., Xiao, Z., & Luo, Y. (2025). Sustainable nanotechnology for food preservation: Synthesis, mechanisms, and applications of zinc oxide nanoparticles. *Journal of Agriculture and Food Research*, 19, 101743. [\[Crossref\]](#)
- Rahman, F., Majed Patwary, M. A., Bakar Siddique, M. A., Bashar, M. S., Haque, M. A., Akter, B., Rashid, R., Haque, M. A., & Royhan Uddin, A. K. M. (2022). Green synthesis of zinc oxide nanoparticles using *Cocos nucifera* leaf extract: Characterization, antimicrobial, antioxidant and photocatalytic activity. *Royal Society Open Science*, 9(11), 220858. [\[Crossref\]](#)
- Salata, O. V. (2004). Applications of nanoparticles in biology and medicine. *Journal of Nanobiotechnology*, 2(1), 3. [\[Crossref\]](#)
- Sharma, S., Singh, S., & Khare, N. (2016). Enhanced photosensitization of zinc oxide nanorods using polyaniline for efficient photocatalytic and photoelectrochemical water splitting. *International Journal of Hydrogen Energy*, 41(46), 21088–21098. [\[Crossref\]](#)
- Srimeena, S., & Nithya, S. (2019). Green synthesis and characterization of zinc oxide nanoparticles using *Cassia articulata* flower extract. *International Journal of Advanced Research*, 7(12), 674–677. [\[Crossref\]](#)
- Tababouchet, M. Y., Sakri, A., Bouremel, C., & Boutarfaia, A. (2023). Synthesis of polyaniline-zinc oxide composites: Assessment of structural, morphological, and electrical properties. *Annales de Chimie: Science des Matériaux*, 47(6), 399–404. [\[Crossref\]](#)
- Turkten, N., Karatas, Y., & Bekbolet, M. (2021). Preparation of PANI modified ZnO composites via different methods: Structural, morphological and photocatalytic properties. *Water*, 13(8), 1025. [\[Crossref\]](#)
- Wang, B., Biesold, G. M., Zhang, M., & Lin, Z. (2021). Amorphous inorganic semiconductors for the development of solar cell, photoelectrocatalytic and photocatalytic applications. *Chemical Society Reviews*, 50(12), 6914–6949. [\[Crossref\]](#)
- Wang, Z., Liu, J., Wang, Y., Sun, H., & Yu, H. (2025). The influence of interface morphology on the interfacial bonding behavior and mechanical properties of TC4/TA2 composite plates. *Materials Science and Engineering: A*, 936, 148401. [\[Crossref\]](#)
- Yahaya, A. A., Umar, A. B., Mamuda, S., & Ahmad, A. M. (2022). Characterization of the structural and optical properties of copper oxide for use in solar cells using screen printing method. *UMYU Scientifica*, 1(1), 184–193. [\[Crossref\]](#)
- Zhanfeng, Q., Guancheng, L., & Xiuli, G. (2025). Multi-element synergy in photocatalytic materials integrated mechanism-design-preparation strategies. *Materials Research Express*, 12(6). [\[Crossref\]](#)
- Zhou, Y. H., Shen, Y. Y., Chen, Y., & Wang, M. H. (2025). Preparation of ZnO/PANI composite by in situ polymerization approach and its varistor properties. *Journal of Materials Science: Materials in Electronics*, 36(16), 965. [\[Crossref\]](#)
- Zhu, C., & Wang, X. (2025). Nanomaterial ZnO synthesis and its photocatalytic applications: A review. *Nanomaterials*, 15(9), 682. [\[Crossref\]](#)